EUROPEAN ORGANIZATION FOR NUCLEAR RESEARCH

CERN-EP/80-83
3 June 1980

DETERMINATION OF THE ABSOLUTE MOMENTUM OF A HIGH-ENERGY HADRON BEAM USING ELASTIC SCATTERING OF HADRONS FROM A HELIUM TARGET

J.P. Burq[*], M. Chemarin[*], M. Chevallier[*], A.S. Denisov[**], T. Ekelöf[***,†], J. Fay[*], P. Grafström[***,†], L. Gustafsson[†], E. Hagberg[†], B. Ille[*], A.P. Kashchuk[**], G.A. Korolev[**], A.V. Kulikov[**], M. Lambert[*], J.P. Martin[***,*], S. Maury[***,††], J.L. Paumier[††], M. Querrou[††], V.A. Schegelsky[**], I.I. Tkach[**], M. Verbeken[††] and A.A. Vorobyov[**]

ABSTRACT

In a small-angle elastic scattering experiment (NA8) in the H8 beam of the CERN Super Proton Synchrotron, the absolute momentum of the incident beam particles has been determined from data on hadron-^{4}He elastic scattering. Measurements were performed at beam momenta ranging from 100 GeV/c to 300 GeV/c, and the average absolute momentum was determined with a precision of 0.15%. This method can be applied also at higher energies.

(Submitted to Nuclear Instruments and Methods)

*) Institut de Physique nucléaire, IN2P3, Université de Lyon-Villeurbanne, France.
**) Leningrad Nuclear Physics Institute, Gatchina, USSR.
***) At present CERN, Geneva, Switzerland.
†) The Gustaf Werner Institute, University of Uppsala, Sweden.
††) Laboratoire de Physique corpusculaire, IN2P3, Université de Clermont-Ferrand, Aubière, France.

1. INTRODUCTION

The aim of the elastic-scattering experiment NA8 at the CERN Super Proton Synchrotron is to measure the differential cross-sections $d\sigma/dt$ for πp small-angle scattering with a precision of 1%. In such measurements it is essential to have a precise absolute calibration of the t-scale, as an error of 1% in this scale would produce an error of the order of 1% in $d\sigma/dt$.

In the experiment, both the scattering angle θ of the forward particle and the kinetic energy T_R of the recoil particle are measured. This provides two independent ways of determining the four-momentum transfer squared t:

$$|t| = (p\theta)^2 \ , \tag{1}$$

$$|t| = 2M_R T_R \ . \tag{2}$$

Here, M_R is the recoil mass and p is the momentum of the beam particle.

A special ionization chamber serves both as a gas target (H_2 or He) and as a recoil detector in the experiment. In this chamber the amount of ionization produced by the recoil is a measure of the recoil energy T_R. A radioactive source emitting α particles of kinetic energy E_α is used to calibrate the T_R scale. Using He as gas filling, the recoiling particles will also be α particles, and for events with $T_R^* = E_\alpha$, the α source signals represent an absolute calibration reference which does not rely on any assumptions about the relation between ionization charge and recoil energy, or about the linearity of the pulse-height registration electronics. This reference for T_R at $T_R^* = E_\alpha$ will in turn provide an absolute reference for a certain value t^* of the four-momentum transfer squared:

$$|t^*| = 2M_\alpha E_\alpha \ . \tag{3}$$

At any fixed value of the beam momentum there will be a certain angle θ^* corresponding to t^*. Knowing this angle, Eq. (1) gives the scaling law which provides an absolute determination of the whole t-scale under the assumption that the θ-scale is strictly linear:

$$t = t^*(\theta/\theta^*)^2 \ . \tag{4}$$

In practice, the value of θ^* was determined from the correlation between θ and T_R in the measured data as the mean scattering angle corresponding to T_R^*. Using Eq. (4), the following relation for the absolute t-scale is obtained:

$$|t| = 2M_\alpha E_\alpha (\theta/\theta^*)^2 \ . \tag{5}$$

Combining Eq. (3) with Eq. (1), we obtain the mean beam momentum as

$$p^* = \frac{\sqrt{2M_\alpha E_\alpha}}{\theta^*} \ , \tag{6}$$

which thus provides an absolute determination of p, if the absolute value of θ^* is known. The accuracy in this p^* determination will therefore essentially only rely on the accuracy of the geometrical determination of the θ-scale.

For the elastic-scattering experiment, the absolute determination of p^* is not necessary as it is enough to know the absolute calibration of the t-scale, according to Eq. (5). However, as in addition the absolute calibration of the θ-scale was known with high precision, an independent determination of p^* was obtained as a by-product in the experiment.

Below we present results of determinations of p^* in a series of different beam momentum settings. These results are compared with the nominal values of the beam momentum p_0 determined from magnetic field measurements of the bending magnets in the beam line.

2. EXPERIMENTAL LAYOUT

The layout of the elastic-scattering experiment is shown in Fig. 1. The experiment was installed in the H8 beam line at the SPS. Here we describe the features of the set-up that are of relevance to the determination of the absolute beam momentum.

2.1 The recoil detector IKAR[1,2)]

The recoil detector is an ionization chamber which, for the purpose of the beam-momentum calibration experiment, was filled with a mixture of He (8 atm) and H_2 (2 atm). Neither of the gases had an impurity content exceeding 10^{-6}. Two of the six separate ionization chamber cells in IKAR are shown in Fig. 2. Each cell

contains an anode plate and a cathode plate, 12 cm apart, mounted perpendicularly to the beam direction. An earthed wire grid is placed 2 cm away from the anode. When an incident beam particle makes an elastic collision with a target ^{4}He nucleus, this nucleus recoils out in a direction almost parallel to the electrode plates, ionizing the gas along its path. The electron track thus created in the gas will start to drift in the high electric field towards the anode plate. The unshielded cathode will feel a signal immediately after the collision as the electrons start to separate from the ions, whereas the anode signal will appear only when the electrons drift through the grid. The electron drift time from cathode to anode is 22 μsec. The anode plate is divided into three electrodes (A, B, and C) that are mounted concentrically around the beam axis.

The recoil kinetic energy T_R was derived from the pulse height of the anode A signal. Recoil particles of ^{4}He in the energy interval 1 MeV $\leq T_R \leq$ 6 MeV were detected. The range of such particles did not reach outside the anode A zone, and anodes B and C were used only to reject long-range background particles. The length of the recoil track projection X_R on the beam axis was obtained from the rise-time of the anode A pulse, as this time is a measure of the inclination of the electron track. Furthermore, the delay of the anode pulse with respect to the passage of the beam particle is a measure of the distance Z_R of the recoil track from the cathode (Fig. 2).

The beam enters and leaves the pressure vessel through steel windows that are 270 μm thick and 80 mm in diameter. In the region where the beam traverses the chamber electrodes, these electrodes are made of thin aluminium foils of a total thickness of 360 μm.

Alpha sources (^{234}U) that had been deposited on each cathode were used for the T_R-scale calibration. In two cells, α sources had been deposited also on the grids with the purpose to control the amount of the electrons lost during their drift in the cathode-grid space. Such losses are the result of adhesion of the electrons to electro-negative impurities such as O_2 contained in the gas mixture.

In the present case the losses due to electron adhesion were about 0.5% per 10 cm drift.

Our studies showed that the ionization produced by the ^{4}He recoils in the He-H_2 mixture is a linear function of their energy:

$$T_R = (V_R - V_0) \frac{E_\alpha}{V_\alpha - V_0} \left[1 - \delta(Z_R)\right] , \tag{7}$$

where

$E_\alpha = (E_\alpha^{(0)} - \Delta_{abs})$ is the α-particle energy corrected for the energy absorption in the matter of the α source, $E_\alpha^{(0)} = 4.777$ MeV;

V_α is the mean amplitude of pulses produced by the α particles from the cathode source;

V_R is the amplitude of the pulse produced by an ^{4}He recoil;

$V_0 = V_\alpha \cdot E_0 / E_\alpha$, $E_0 = 40$ keV;

$\delta(Z_R)$ is a correction which takes into account both the loss of electrons through adhesion and the limited transparency of the grid.

As the adhesion of the electrons could be measured and controlled, $\delta(Z_R)$ is a known function of Z_R. In the present case, the correction was

$$\delta(Z_R) \simeq 0.05\% \cdot Z_R(\text{cm}) \quad \text{for} \quad Z_R \leq 5 \text{ cm} . \tag{8}$$

Only recoils produced close to the cathode ($1 \leq Z_R \leq 2$ cm) were used for the calibration, and the $\delta(Z_R)$ correction therefore did not exceed 0.1%.

The absorption in the α sources was determined experimentally by analysing the angular dependence of the mean value of the α-pulse amplitude $V_\alpha(\phi)$, where ϕ is the angle between the α track and the direction perpendicular to the electrodes. In practice, α particles emitted at $\phi \simeq 70^\circ$ were used for the T_R-scale calibration. The absorption correction at this angle averaged over all the chamber cells was found to be

$$\Delta_{abs} = 10 \text{ keV} \pm 5 \text{ keV} .$$

From these considerations the total error in the absolute measurements of the recoil energies around $T_R^* = E_\alpha$ may be estimated to be $\sigma_{T_R} = 0.1\%$.

Each beam particle produces ionization in the sensitive volume of IKAR, which might cause some small shift in the measured recoil energies. However, this effect was eliminated by sending an electronically generated compensation pulse, synchronized with each beam particle, to the amplifiers. The fluctuations of the ionization produced by the beam particles determined the energy resolution of IKAR at high beam intensities. At a beam intensity of 10^6 particles per 1 s spill the resolution was 130 keV (FWHM).

2.2 The forward spectrometer

This spectrometer served to determine the scattering angle θ and the momentum p_{out} of the forward scattered particles. Six blocks (PC1-PC6) of multiwire proportional chambers (MWPCs) were used to measure the horizontal (x_1-x_6) and vertical (y_1-y_5) coordinates of the forward particle. The values of θ and p_{out} were obtained using the following relations:

$$\theta^2 = \theta_x^2 + \theta_y^2 - 2\sigma_{\theta_{proj}}^2 \tag{9}$$

$$\theta_x = \frac{x_4 - x_3}{L_2} - \frac{x_2 - x_1}{L_1}$$

$$\theta_y = \frac{y_4 - y_3}{L_2} - \frac{y_2 - y_1}{L_1} \tag{10}$$

$$p_{out}^{-1} = \text{const} \left(\frac{x_6 - x_5}{L_3} - \frac{x_4 - x_3}{L_2} \right) . \tag{11}$$

Here, $\sigma_{\theta_{proj}}$ is the angular resolution of the forward spectrometer; L_1, L_2, L_3 are the distances between the PC1-PC2, PC3-PC4, and PC5-PC6 blocks, respectively. For the bending magnets Bend 5-Bend 8, no absolute magnetic field calibration had been made and the measurements of p_{out} were thus relative. This measurement was used to reduce the background of inelastic scattering.

Blocks PC1, PC2, and PC3 contained four MWPCs each (two chambers in the X-plane and two chambers in the Y-plane) and block PC4 contained six such chambers.

The wire spacing in all MWPCs was 1 mm. All these chambers were tilted around the central wire by an angle $\psi \approx 10^\circ$ with respect to the beam direction. This increased the probability for a two-wire hit to about 50%, which had the effect of improving the spatial resolution (FWHM) of the chambers by a factor of two[3]. Furthermore, adjacent chambers with parallel wires were shifted by 0.25 mm with respect to each other. It should be noted that with inclined MWPCs the coordinates (x_i, y_i) entering in Eqs. (10) and (11) are determined as

$$x_i = x_i' \cos \psi_i \ , \tag{12}$$

where x_i' is the coordinate given by the MWPC read-out system. Block PC5 contained six X chambers and two Y chambers, while block PC6 contained only two X chambers. The useful areas of the chambers were 32 × 32 mm^2 in PC1 and PC2, 48 × 48 mm^2 in PC3, 160 × 160 mm^2 in PC4, 192 × 192 mm^2 in PC5, and 287 × 287 mm^2 in PC6. The alignment of all the MWPCs was performed using beam particles, and the resulting precision was better than 50 μm. The angular acceptance of the forward spectrometer was close to 100% for the t-range under investigation.

In order to minimize hadronic interactions of the beam particles with the air and to reduce the multiple Coulomb scattering, vacuum tubes were used between the MWPC blocks. For the same purposes, a He bag was used inside the magnets Bend 5-Bend 8. The momentum resolution of the forward spectrometer was $\sigma_{p_{out}}/p_{out}$ = = 0.2-0.3%. The resolution in the projected forward scattering angle measurements varied from $\sigma_{\theta_{proj}}$ = 32 μrad at p = 100 GeV/c to $\sigma_{\theta_{proj}}$ = 18 μrad at p = 300 GeV/c.

The error in the absolute value of the scattering angle was dominated by the uncertainties in the wire spacings of the MWPCs in block 4. Special microscopic measurements of the wire spacing in two 100 × 100 mm^2 chambers and in one 200 × × 200 mm^2 chamber showed that the systematic deviation of the mean wire spacing from the nominal value did not exceed ±0.1%. The distances L_1 and L_2, which were about 20 m each, were measured with a precision of ±1 mm. The relative effect of this error is negligible in comparison with the previous one. Also, the inclination angle $\psi \approx 10^\circ$ was known with a precision of ±2 mrad, and the corresponding

contribution to σ_θ/θ was only on the level of 3×10^{-4}. From this it follows that the error in the absolute measurement of the scattering angle was $\sigma_\theta/\theta \simeq \pm 0.1\%$.

3. MEASUREMENTS AND RESULTS

The secondary beam used in the experiment was derived from a 400 GeV primary proton beam. The high-resolution beam spectrometer, provided in the incident beam as a general facility, gave information on the momentum of each beam particle within the momentum bite defined by the momentum slit (Fig. 1). During the experiment the width of this slit was varied in order to maintain the intensity in the secondary beam line at a constant level, and as a result the momentum bite varied between $\Delta p = \pm 0.2\%$ and $\Delta p = \pm 1\%$. The collimator was opened symmetrically in order to keep the mean value of the momentum close to the nominal value. The mean values of the momentum as measured with the beam spectrometer proved to be equal to the nominal value p_0 within $\pm 0.05\%$.

The beam was focused onto IKAR, and the dimensions of the beam spot at focus were about 10×10 mm^2. The intensity of the beam was 8×10^5 particles over an effective spill length of 800 ms, and the burst cycle time was 10.8 s.

The trigger was formed on three sequential levels. The first-level trigger $S1A \cdot S1B \cdot (S2A \cup S2B) \cdot \overline{A1} \cdot \overline{A2} \cdot \overline{A3}$ defined an incident particle traversing IKAR inside the beam channel. It also eliminated part of the inelastic scatterings. A trigger was not accepted if another beam particle arrived within 80 ns of the first. The first-level trigger strobed PC1–PC4 and gave a start signal to a Special Digital Processor Unit (SDPU) [4]. The SDPU received information from PC1, PC2, and PC4, and calculated within 250 ns whether or not the scattering angle was bigger than a preset threshold value. If this was the case, a second-level trigger was produced. With a threshold value corresponding to $t = 3 \times 10^{-3}$ GeV^2 the reduction in the trigger rate due to the SDPU was around a factor of 250.

The second-level trigger strobed the MWPCs in blocks PC5, PC6, BS1–BS4, and opened the gates of the IKAR shapers. If a cathode signal arrived within 4 μs

and an anode signal arrived within 25 μs, the data acquisition system was triggered. The reduction in the trigger rate due to this third-level trigger requirement was about a factor of 25, and as a result about 100 events were sent on tape every burst. These events contained about 30 elastic scatterings having a recoil energy of 1 MeV $\leq T_R \leq$ 6 MeV and longitudinal track positions of 1 cm $\leq Z_R \leq$ 9 cm.

In the data analysis, the events were first selected using the following criteria:

i) the forward particle track should be reconstructible in each PC block;

ii) the forward particle should be neither a muon nor an electron;

iii) the momentum of the scattered particle should be within ±5% of the momentum of the incident beam;

iv) there should be no detectable pulses on the electrodes B and C of IKAR;

v) the longitudinal recoil track position should be within 1 cm $\leq Z_R \leq$ 9 cm.

Most of the events selected with such requirements are elastic scatterings, as can be seen from Figs. 3 and 4, where correlation matrices of T_R versus X_R and of T_R versus the difference $\Delta = \left[(p_0\theta)^2/2M_R - T_R\right]$ are presented for $\pi^- - {}^4He$ scattering at p_0 = 250 GeV/c. The final selection was performed cutting the tails in these two-dimensional distributions. This was done using the χ^2-distribution method.

Figure 5 shows the distributions of $p-p_{out}$ for selected events. The essential part of the comparatively small tails of the distribution is due to bremsstrahlung of the scattering particles. From Figs. 3 to 5 we conclude that the selection of the elastic events is satisfactory.

For the determination of the absolute value of the incident particle momentum, only events with a recoil energy close to E_α = 4.77 MeV were used (4.26 MeV $\leq T_R \leq$ $\leq$ 5.26 MeV). A further requirement was that the recoil track should be positioned near the cathode (1 cm $\leq Z_R \leq$ 2 cm). For events selected in this way, the distribution of the difference $\Delta = \left[(p_0\theta)^2/2M_R - T_R\right]$ is shown in Fig. 6. From this figure it follows that the momentum transfer squared determined from the scattering angle,

assumping $p = p_0 = 250.0$ GeV/c, proved to be slightly lower than that determined from the recoil energy. The corrected value p^* of the incident momentum is:

$$p^* = p_0 \left(1 - \frac{\bar{\Delta}}{2E_\alpha}\right) .$$

At 250 GeV/c

$$\frac{p^* - p_0}{p_0} = - \frac{\bar{\Delta}}{2E_\alpha} = (+0.15 \pm 0.05)\% .$$

was obtained. The results for the other beam momenta are given in Table 1. The errors given in this table are statistical only.

The systematic error due to the uncertainty in θ is ±0.1%, and that due to the limited precision in T_R is ±0.05%. These errors can be assumed to be the same in the different measurements and therefore represent a possible common shift in all measured momenta.

In conclusion the described method provided a determination of the absolute momentum of the hadron beam with a precision of ±0.15%. There is no foreseeable limitation in the application of the method when going to higher energies.

The assistance given by the SPS Experimental Area Group at CERN is gratefully acknowledged. In particular, we would like to thank the persons who helped us with the beam tuning, with the use of the beam spectrometer, and with the geometrical alignment of the experiment.

REFERENCES

1) A.A. Vorobyov et al., Nucl. Instrum. Methods 119, 509 (1974).

2) J.P. Burq et al., Phys. Lett. 77B, 438 (1978).

3) E.A. Damaskinsky et al., Nucl. Instrum. Methods 130, 611 (1975).

4) A.P. Kashchuk and V.L. Golovtsov, Leningrad Nuclear Physics Institute, Gatchina Report 395 (1978).

Table 1

Polarity	p_0 (GeV/c)	$\frac{p^* - p_0}{p_0}$ (%)	p^* (GeV/c)
–	100	+0.30 ± 0.05	100.30 ± 0.05
+	100	+0.20 ± 0.05	100.20 ± 0.05
–	150	+0.35 ± 0.12	150.52 ± 0.18
+	150	+0.35 ± 0.05	150.52 ± 0.08
–	200	+0.35 ± 0.06	200.79 ± 0.12
–	250	+0.15 ± 0.05	250.38 ± 0.13
+	250	+0.15 ± 0.07	250.38 ± 0.18
–	280	+0.23 ± 0.10	280.64 ± 0.28
–	300	−0.04 ± 0.06	299.88 ± 0.18
+	300	−0.08 ± 0.06	299.76 ± 0.18

Figure captions

Fig. 1 : Layout of the experiment: B1-B8 are bending magnets; CED1, CED2 are differential Čerenkov counters; TH1, TH2 are threshold Čerenkov counters; BS1-BS4 are multiwire proportional chambers of the beam spectrometer; PC1-PC6 are blocks of multiwire proportional chambers; S1-S2, A1-A3 are scintillator counters; and IKAR is the recoil detector. In the beam layout all quadrupoles and correction dipoles and all collimators except the momentum-defining slit have been omitted.

Fig. 2 : The recoil detector IKAR. The upper picture shows schematically the construction of two cells of IKAR, and the diagrams below show the pulses produced on the electrodes by a recoil particle in the gas; d is the cathode-grid distance and W is the drift velocity of the electrons in the gas.

Fig. 3 : Plot showing the correlation between the recoil energy T_R and the length X_R of the recoil track projection on the beam axis for a sample of elastic events that have passed a preliminary selection.

Fig. 4 : Plot showing the correlation between the recoil energy T_R and the difference $\Delta = (p_0\theta)^2/2M_R - T_R$ between recoil energy for elastic events as measured by the forward spectrometer and as measured by recoil detector, for a sample of events that have passed a preliminary selection.

Fig. 5 : Plot showing the momentum distribution of elastically scattered pions after the final selection of the elastic events.

Fig. 6 : Distribution showing the difference $\Delta = (p_0\theta)^2/2M_R - T_R$ for elastic events that satisfy the requirements: $4.26\ \text{MeV} \leq T_R \leq 5.26\ \text{MeV}$, and $1\ \text{cm} \leq Z_R \leq 2\ \text{cm}$. The curve represents a fit of a Gaussian to the data. The resulting values of the mean value $\bar{\Delta}$ and of χ^2/N are indicated in the figure.

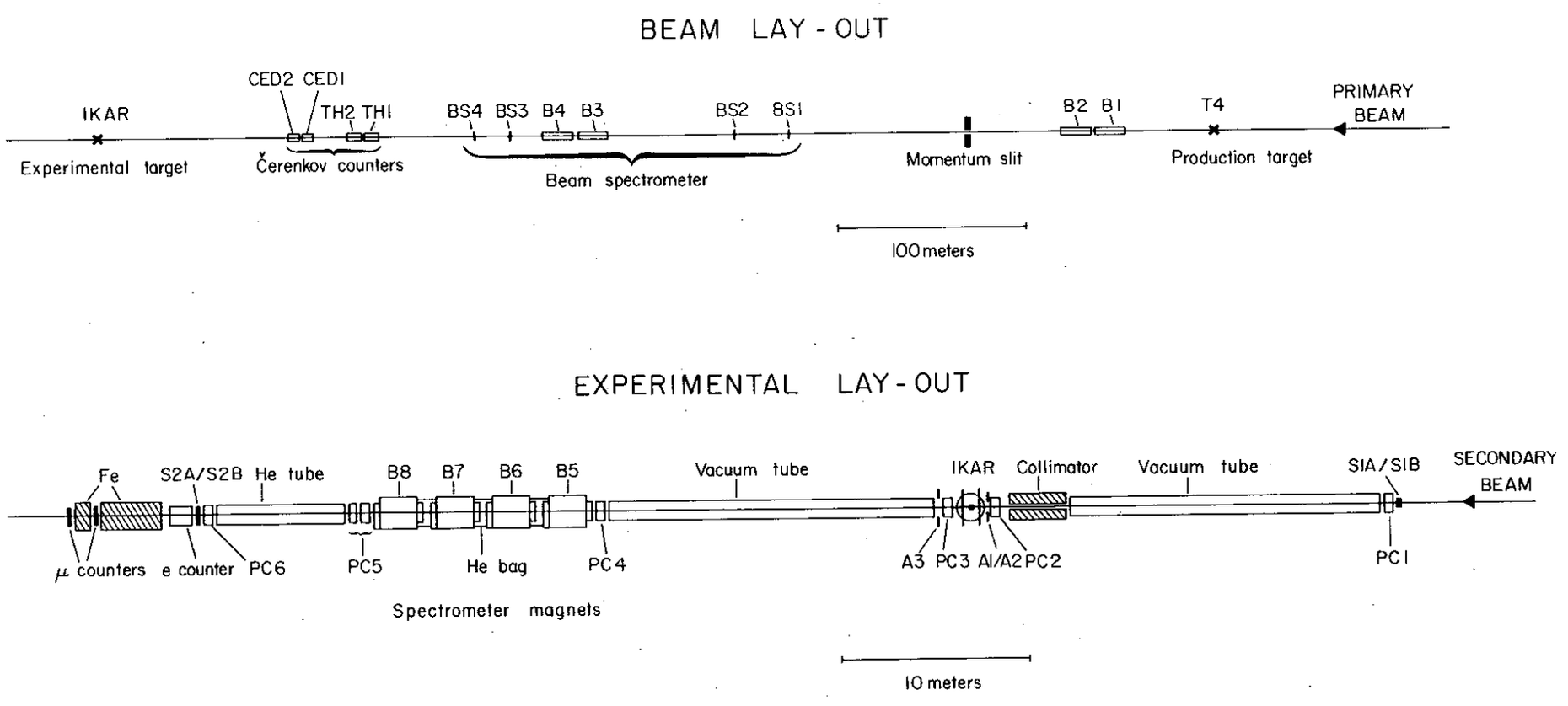
BEAM LAY-OUT
IKAR
CED2 CED1
TH2 THI
BS4 BS3 B4 B3
BS2 BS1
B2 B1
T4
PRIMARY BEAM
Experimental target
Čerenkov counters
Beam spectrometer
Momentum slit
Production target
100 meters
EXPERIMENTAL LAY-OUT
Fe
S2A/S2B
He tube
B8 B7 B6 B5
Vacuum tube
IKAR
Collimator
Vacuum tube
SIA/SIB
SECONDARY BEAM
μ counters
e counter
PC6
PC5
He bag
PC4
A3 PC3 AI/A2 PC2
PC1
Spectrometer magnets
10 meters

Fig. 1

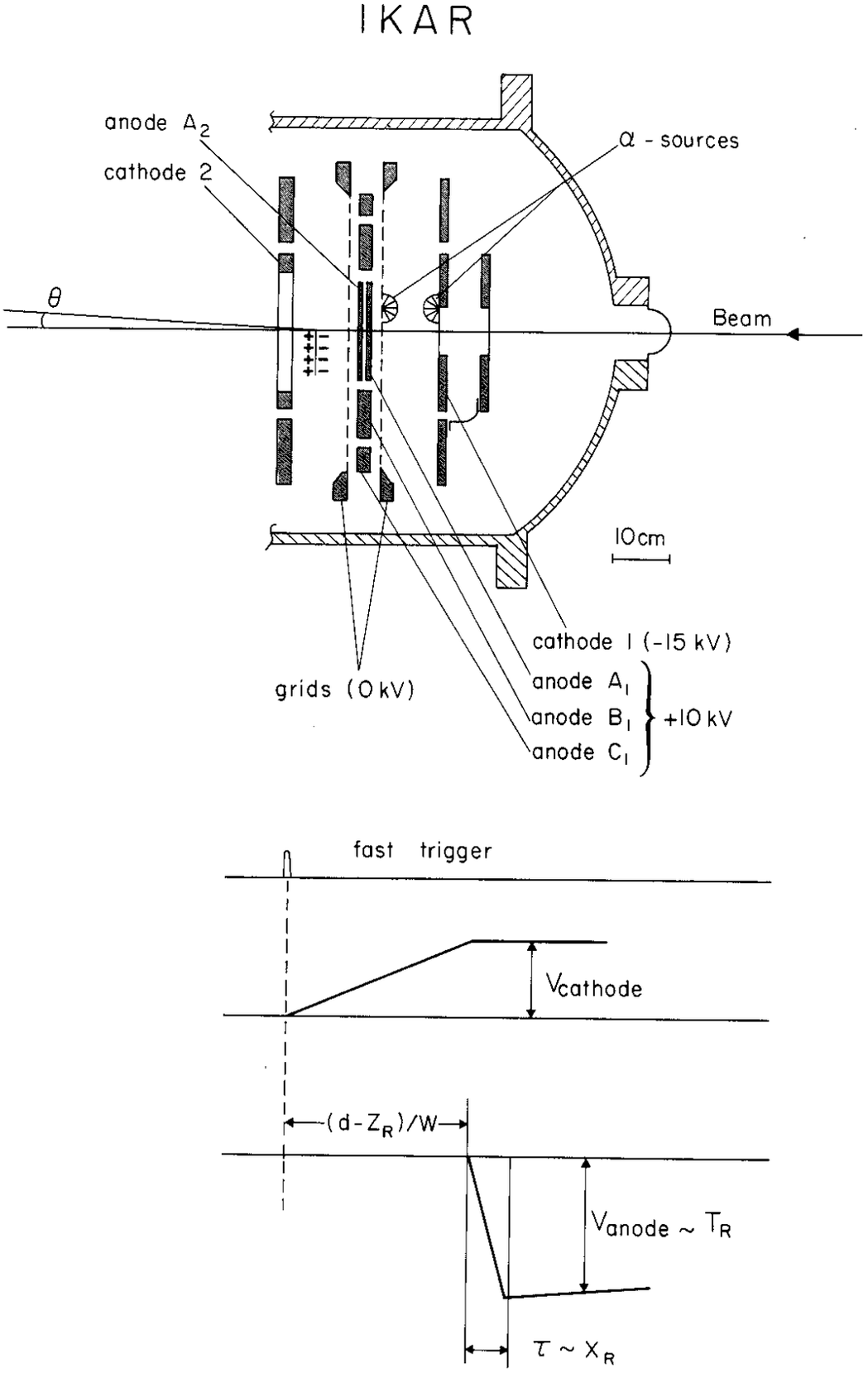
IKAR
anode A_2
cathode 2
α - sources
θ
Beam
10cm
cathode 1 (-15 kV)
grids (0 kV)
anode A_1
anode B_1
anode C_1
+10 kV
fast trigger
$V_{cathode}$
$(d-Z_R)/W$
$V_{anode} \sim T_R$
$\tau \sim X_R$

Fig. 2

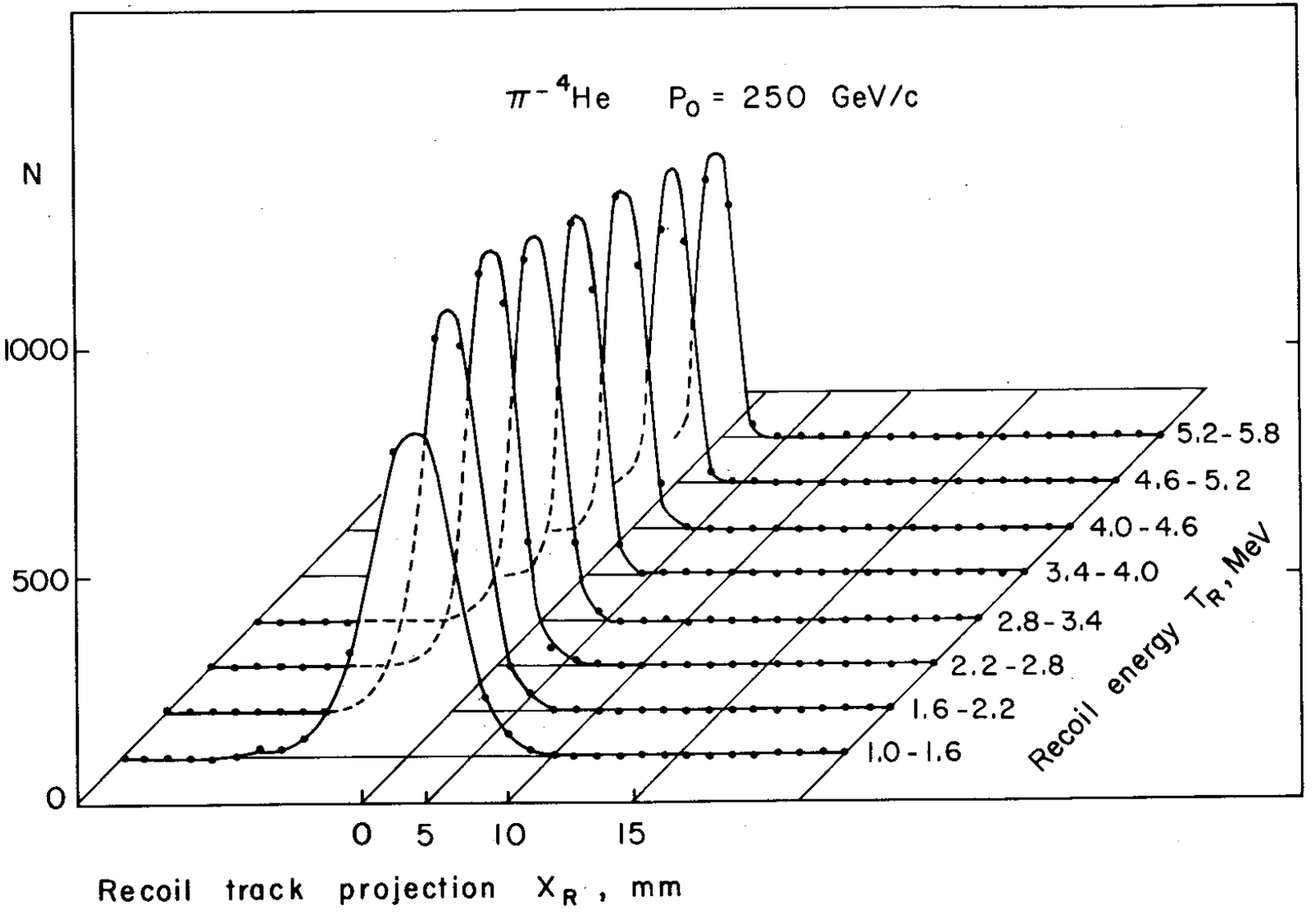
$\pi^- {}^4He$ P_0 = 250 GeV/c
N
1000
500
0
0 5 10 15
Recoil track projection X_R, mm
5.2-5.8
4.6-5.2
4.0-4.6
3.4-4.0
2.8-3.4
2.2-2.8
1.6-2.2
1.0-1.6
Recoil energy T_R, MeV

Fig. 3

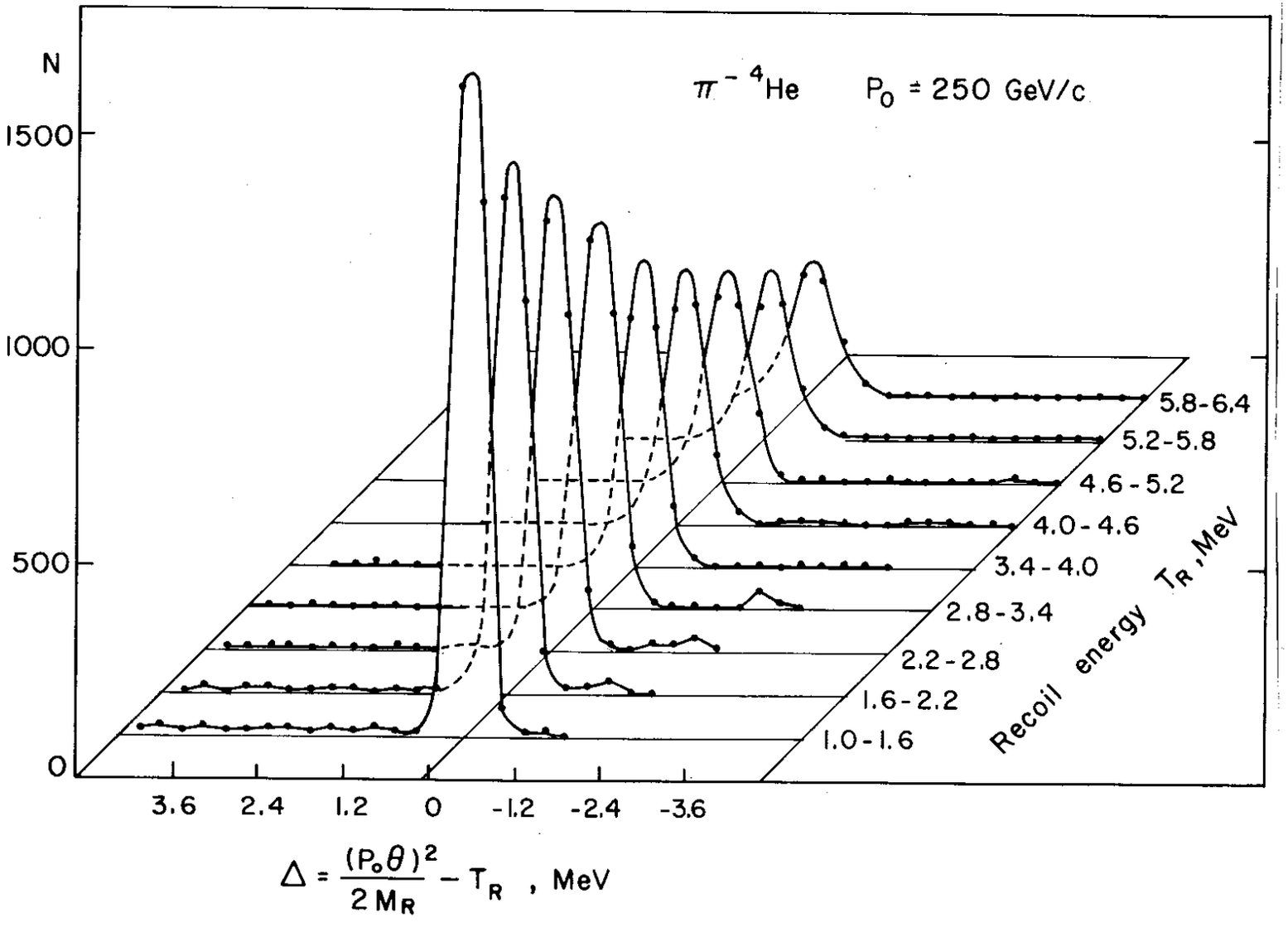
N
1500
1000
500
0
$\pi^- {}^4He$ P_0 = 250 GeV/c
5.8-6.4
5.2-5.8
4.6-5.2
4.0-4.6
3.4-4.0
2.8-3.4
2.2-2.8
1.6-2.2
1.0-1.6
Recoil energy T_R, MeV
3.6
2.4
1.2
0
-1.2
-2.4
-3.6
$\Delta = \frac{(P_0\theta)^2}{2M_R} - T_R$, MeV

Fig. 4

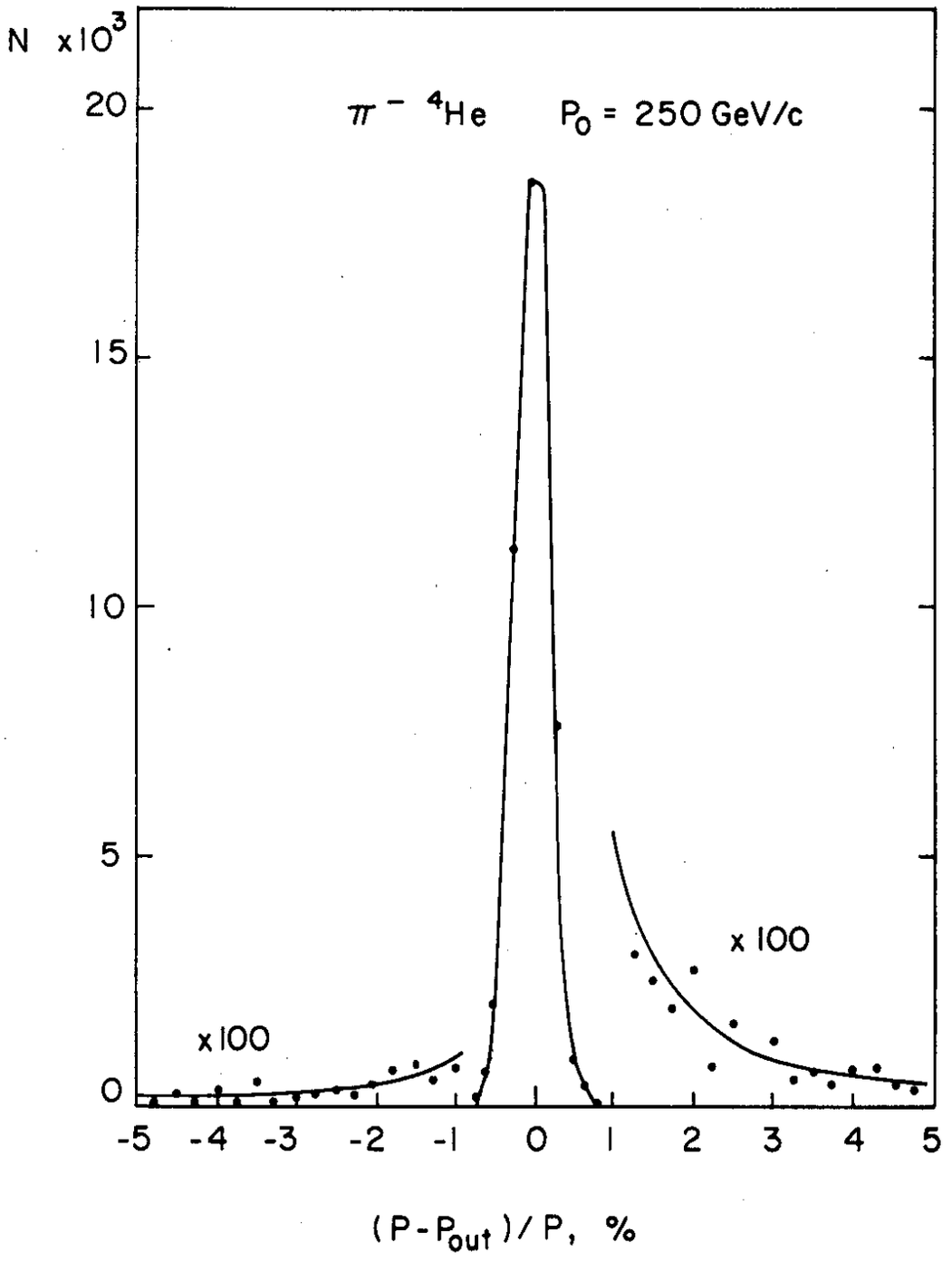
N x10^3
20
15
10
5
0
π⁻ ⁴He P₀ = 250 GeV/c
x 100
x 100
-5 -4 -3 -2 -1 0 1 2 3 4 5
(P-P_out)/P, %

Fig. 5

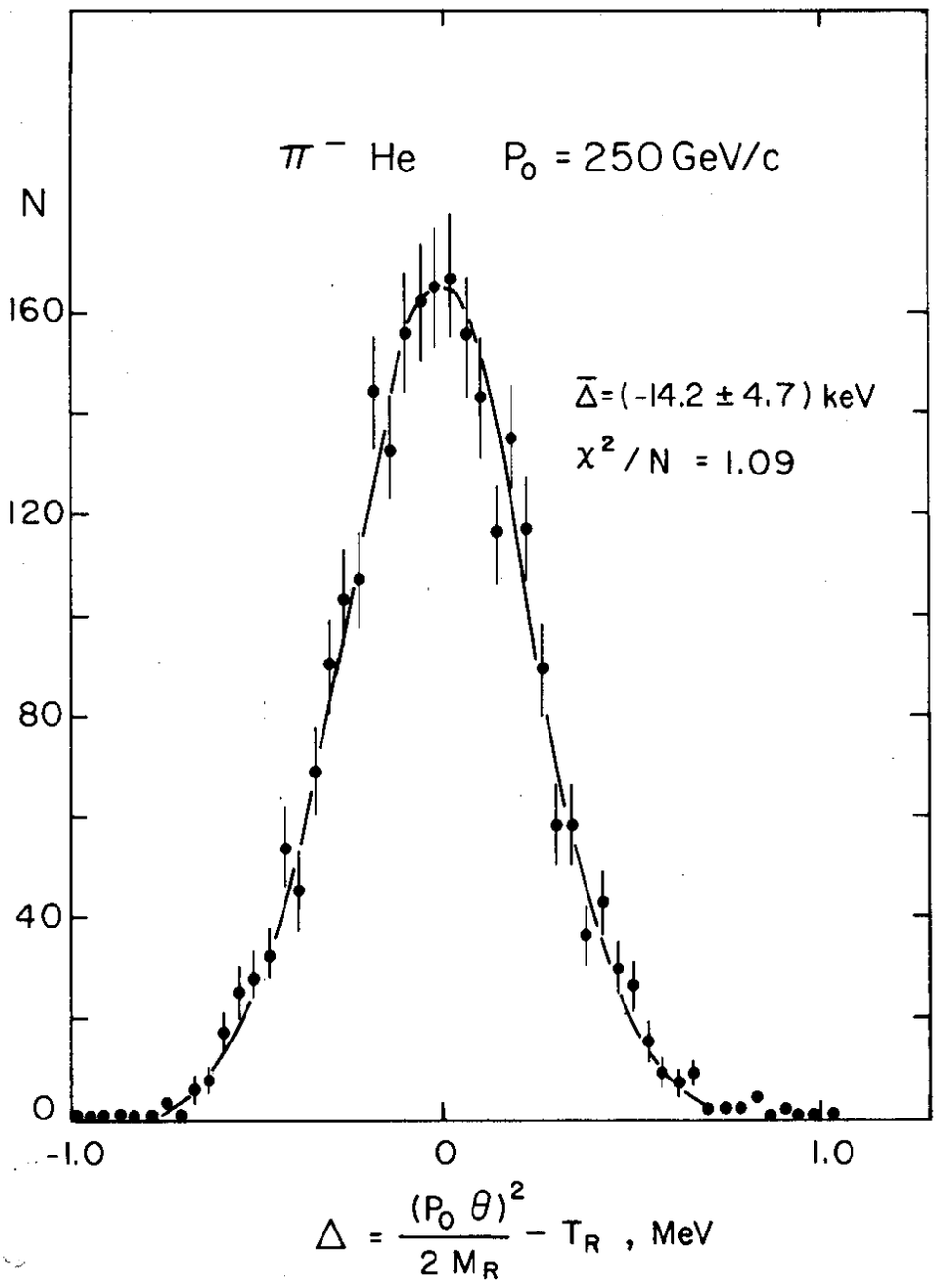
π^- He P_0 = 250 GeV/c
N
160
120
80
40
0
-1.0
0
1.0
$\bar{\Delta}$=(-14.2 ± 4.7) keV
χ^2 / N = 1.09
$\Delta = \frac{(P_0\,\theta)^2}{2\,M_R} - T_R$, MeV

Fig. 6